Biochemistry

 Volume 32, Number 22 June 8, 1993

Articles

Photoaffinity Labeling of Skeletal Myosin with 2-Azidoadenosine Triphosphate†

Jean C. Grammer, Hideto Kuwayama,‡ and Ralph G. Yount*

Department of Biochemistry and Biophysics and Department of Chemistry, Washington State University, Pullman, Washington 99164-4660

Received February 4, 1993; Revised Manuscript Received March 23, 1993

ABSTRACT: The purine binding site of ATP on skeletal muscle myosin has been photoaffinity labeled with 2-azidoadenosine diphosphate (2-N_3ADP). 2-N_3ADP was stably trapped at the active site ($t_{1/2} \sim 5$ days, 0 °C) by complexation of the two heavy chain reactive thiols (Cys-697 and Cys-707) with Co(III)phenanthroline. Photoincorporation occurred only in the 23-kDa NH_2-terminal tryptic fragment of the heavy chain. Extensive serial digestion of photolabeled subfragment 1 of myosin by trypsin and subtilisin yielded a series of labeled peptides which were purified by HPLC. Sequence and radiolabeling analysis of eight photolabeled peptides all indicated that tryptophan-130 was the only labeled residue. This site of labeling confirms earlier photolabeling studies with the non-nucleotide ADP analogue, 2-[(4-azido-2-nitrophenyl)-amino]ethyl diphosphate (NANDP), which also labeled Trp-130 [Okamoto, Y., & Yount, R. G. (1985) *Proc. Natl. Acad. Sci. U.S.A. 82*, 1575–1579]. Comparison of the structures of 2-N_3ADP and NANDP indicate that their azido groups can be superimposed if both analogues bind to the active site in an extended conformation in a manner analogous to the *anti* conformation of ATP.

The characterization of the active site of myosin is a key step necessary to understand the molecular basis of how the chemical energy of ATP is transduced into the mechanical energy of muscle contraction. Toward this end we and others have been using photoreactive analogues of ATP to identify amino acid residues and specific regions of the myosin heavy chain which interact with ATP (Okamoto & Yount, 1985; Mahmood et al., 1989; Sutoh, 1987; Cole & Yount, 1990; Garabedian & Yount, 1990, 1991; Atkinson et al., 1986; Maruta et al., 1989; Kerwin & Yount, 1992). These studies have identified amino acids which are at or near the adenine and ribose rings and, by vanadate photochemistry (Grammer et al., 1988; Cremo et al., 1989; Grammer & Yount, 1991), near the γ-phosphate binding site of ATP [reviewed in Yount et al. (1992)].

The first amino acid residue to be identified near the adenine-binding site of myosin was Trp-130 (Okamoto & Yount, 1985). This residue was specifically photolabeled by the arylazido-ADP analogue NANDP.[1] The specificity and extent of photolabeling was enhanced by first trapping NANDP at the active site by cross-linking Cys-707 (SH_1) and Cys-697 (SH_2) with bifunctional thiol reagents (Wells & Yount, 1979, 1982). This cross-linking reaction was shown to stabilize the Mg·NANDP–S1 complex ($t_{1/2} \sim 5$ days at 0 °C) such that the excess NANDP could be removed by gel filtration before photolysis was initiated. Up to 50% of the S1 trapped complex was photolabeled, and all the label was found in the NH_2-terminal 23-kDa tryptic fragment of the heavy chain which contains Trp-130. Moreover, NANTP has been shown to support tension development in skinned fibers almost as well as ATP so that it must bind in a manner analogous to ATP (Pate et al., 1991). Thus, all indications are that the photolabeling of Trp-130 is specific and reflects the fact that this

†Supported by grants from the NIH (DK05195) and the Muscular Dystrophy Association.

‡Current address: Chemistry Department, Obihiro University of Agriculture and Veterinary Medicine, Obihiro, Hokkaido, Japan.

[1] Abbreviations: NANDP, 2-[(4-azido-2-nitrophenyl)amino]ethyl diphosphate; 2-N_3ADP and 2-N_3ATP, 2-azidoadenosine di- and triphosphates, respectively; S1, myosin subfragment 1; 8-N_3ADP and 8-N_3ATP, 8-azidoadenosine di- and triphosphate, respectively. DHNBS, dimethyl(2-hydroxy-5-nitrobenzyl)sulfonium bromide.

0006-2960/93/0432-5725$04.00/0

residue provides part of the adenine-binding site of myosin for ATP.

Recently, chemical modification studies of myosin with the tryptophan reagent DHNBS have shown Trp-130 is the most reactive of the five tryptophans in S1 (Werber et al., 1987; Peyser et al., 1990). Surprisingly, this modification had little effect on the actin-activated MgATPase activity of S1. These observations suggested that NANDP may simply be photolabeling the most reactive tryptophan, which may or may not be at the active site. It was of interest then to verify our earlier results with a different ATP analogue, preferably one more structurally analogous to ATP. Two such azido analogues of ATP exist, 8-N_3ATP (Haley & Hoffman, 1974) and 2-N_3ATP (Czarnecki et al., 1982; Czarnecki, 1984). These two analogues have been used extensively subsequently to photolabel a variety of ATP-binding proteins. For example, with myosin, fluorescent derivatives of 8-N_3ATP have been used to implicate both the COOH-terminal 20-kDa and to a lesser extent the central 50-kDa tryptic fragments of the S1 heavy chain as making up part of the ATP-binding site (Maruta et al., 1989). However, in our hands, 8-N_3ATP labels only the 23-kDa NH_2-terminal tryptic fragment if it is first trapped by crosslinking SH_1 and SH_2 (J. C. Grammer, unpublished results). Identification of labeled residues has been impossible thus far because the percent incorporation is low (2–3%) and the photolabeled residues are unstable to normal peptide purification procedures (Bridenbaugh, 1980; J. C. Grammer, unpublished results).

In contrast, as shown here, about 30% of trapped 2-N_3ADP is photoincorporated into S1, and the photolabeled products are stable to a variety of purification conditions. This stability has allowed several photolabeled active site peptides to be isolated and characterized. All of these peptides showed the only photolabeled amino acid was Trp-130, a result consistent with our earlier NANDP photolabeling results. The fact that these two structurally disparate analogues photolabeled the same Trp residue was surprising but can be explained if both analogues bind to the active site in an extended (*anti*) conformation. These conformations place the azido groups of both analogues in similar positions in the binding site, a situation which rationalizes both the specificity and location of the photolabeling reactions. These results then confirm and extend our earlier studies and strongly implicate Trp-130 as part of the adenine ring binding site of skeletal myosin.

MATERIALS AND METHODS

Chemicals. The commercial compounds and their sources were as follows: Li_3ADP (Pharmacia P-L Biochemicals); [^{3}H]2-chloroadenosine (Moravek Radiochemicals, Brea, CA); 2-chloroadenosine, TPCK trypsin, subtilisin BPN′ (Sigma); ultrapure ammonium sulfate (ICN-Schwarz Mann); acrylamide, bisacrylamide (Kodak); and SDS (Pierce). [^{3}H]2-N_3ADP was synthesized as previously described (Riquelme & Czarnecki, 1983) and its concentration determined using $\epsilon^{M}_{271\ nm}$ of 15 300 M^{-1} cm^{-1} in 0.1 N HCl. [Co(III)(phen)$_2$-CO_3]Cl was synthesized as described (Wells et al., 1979b).

Enzyme Preparations. Rabbit skeletal myosin was prepared according to Wagner and Yount (1975). Myosin was stored in 0.3 M KCl and 50% glycerol at -20 °C. Chymotryptic S1 (115 000 g/mol) was prepared from filamentous myosin as described by Okamoto and Sekine (1985) with the following modifications; the myosin was dialyzed overnight against 0.12 M NaCl and 10 mM phosphate, pH 7.1, at 4 °C and made 1 mM in EDTA just prior to the addition of chymotrypsin; the S1 precipitated by ammonium sulfate was resuspended in S1 buffer containing 0.2 mg/mL phenylmethanesulfonyl fluoride prior to gel filtration to inactivate traces of chymotrypsin which slowly reactivate after ammonium sulfate treatment.

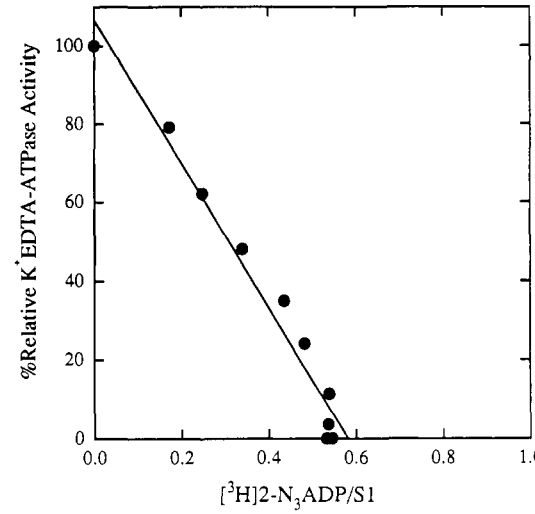

FIGURE 1: Percent K$^+$EDTA ATPase activity vs [^{3}H]2-N_3ADP trapped per S1. S1 (20 μM) was inactivated with the Cophen system as described under Materials and Methods except that, at various times during the inactivation, aliquots were removed and quenched by the addition of 0.5 M EDTA (pH 8.0) to a final concentration of 20 mM. K$^+$EDTA-ATPase activities were assayed at each time point. The remainder of the sample was purified, and the [^{3}H]2-N_3ADP trapped was determined as described under Materials and Methods. The line is the best fit by linear regression analysis.

Enzyme Inactivations and Purifications. To ensure that the [^{3}H]2-N_3ADP was in the photolabile azido tautomeric form (Czarnecki, 1984), the [^{3}H]2-N_3ADP was incubated in 0.1 N HCl for 40 min at room temperature and neutralized with 0.1 M Tris base immediately prior to use. S1 (17–26 μM) in 50 mM Tris and 0.1 M KCl, pH 8.0 (S1 buffer), was inactivated in the presence of 0.2–0.26 mM $MgCl_2$ and 25–60 μM [^{3}H]2-N_3ADP, with a 10-fold molar excess of Co(II)-phenanthroline and a 100-fold molar excess of [Co(III)(phen)$_2$$CO_3$]Cl over S1 for 20 min at 4 °C (Wells & Yount, 1982). Inactivations were quenched by addition of 0.5 M EDTA (pH 8.0) to 20 mM. A 50-fold excess of ATP over 2-N_3ADP was added, and S1 was precipitated by addition of saturated $(NH_4)_2SO_4$ to 66% saturation in the presence of 20 mM EDTA. The pellets from low-speed centrifugation were resuspended in S1 buffer and centrifuged through Sephadex G50 spin columns (Cole & Yount, 1990) equilibrated in S1 buffer to remove $(NH_4)_2SO_4$ and traces of free [^{3}H]2-N_3ADP.

Enzyme Irradiation. S1·[^{3}H]2-N_3ADP solutions were placed in appropriate diameter Pyrex dishes on ice to give a solution depth of 0.5 cm, covered with Pyrex petri dish covers, and irradiated with a Hanovia 450-W medium-pressure Hg lamp (Ace Glass) at a distance of 9 cm. A second Pyrex petri dish cover was used to reduce radiation below 300 nm.

Analytical Procedures. Concentrations of modified S1 were determined by a dye binding assay (Bradford, 1976) using unmodified S1 as the standard as previously described (Wells et al., 1979a); $\epsilon^{1\%}_{280}$ = 7.5 cm^{-1} (Wagner & Weeds, 1977). ATPase assays were performed as previously described (Wells et al., 1979a) except that the release of P_i was measured after 2 and 8 min. Radioactivity was determined in either a Beckman LS 7500 or Packard 1900CA scintillation counter using either ACS or BCS (Amersham) as the scintillant.

Proteolytic Digestion, Purification of Labeled Peptides, and Sequence Analysis. [^{3}H]2-N_3ADP-labeled S1 in S1

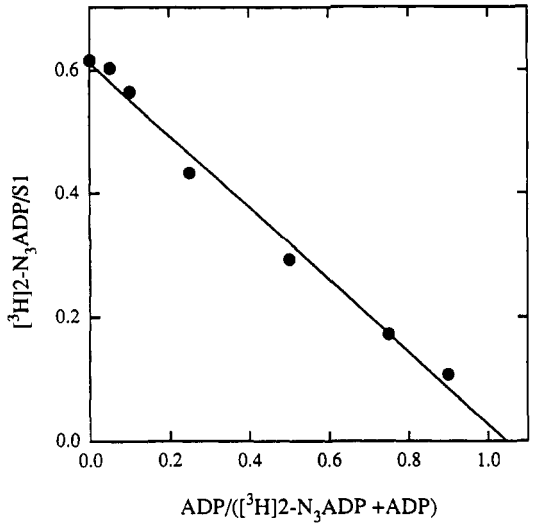

FIGURE 2: Competition of ADP and [^{3}H]2-N_3ADP for trapping on S1. S1 (19.8 μM) was inactivated as described under Materials and Methods using a 1.5-fold molar excess of [^{3}H]2-N_3ADP and varying concentrations of ADP to give the indicated ratios. Samples were quenched with EDTA (Figure 1) after 20 min of incubation, and the trapping stoichiometry was determined as described under Materials and Methods.

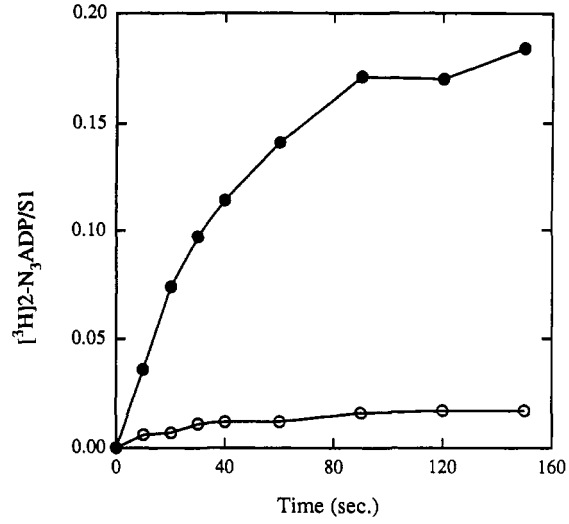

FIGURE 3: Photoincorporation of [^{3}H]2-N_3ADP into S1. (●) The S1·Mg[^{3}H]2-N_3ADP complex (17.6 μM) was prepared and irradiated as described under Materials and Methods. At various times during the irradiation, duplicate samples were removed and precipitated by the addition of an equal volume of cold 10% TCA. The pellets were rinsed once with 5% TCA and solubilized in 2% SDS. After neutralization with 1 M Tris (free base), the samples were counted as described under Materials and Methods. (○) Same as above except no [$Co(III)(phen)_2CO_3]^+$ was added.

buffer (4 mg/mL) was digested with trypsin (1/100, w/w) for 30 min at 25 °C, adjusted to pH 7.8 by the addition of solid NH_4HCO_3, and further incubated with subtilisin BPN′ (1/50, w/w) at 37 °C. After 4 h, the digest was made 2 M in urea, and a second addition of subtilisin (1/50, w/w) was added and digestion allowed to proceed for an additional 4 h. The peptide digest was filtered through a 0.45-μm Nylon-66 filter (Rainin, Inc.) and separated by HPLC using Brownlee RP300 C8 semipreparative (7 mm × 25 cm) and analytical columns (4.6 mm × 13 cm) and a Brownlee AX300 analytical column (4.6 mm × 13 cm). The HPLC system was either a microprocessor controlled Altex/Beckman dual pump set-up connected to a Beckman model 165 dual wavelength detector (semipreparative separations) or a dual pump Rainin system connected to a Waters 991 photodiode array detector (analytical separations).

Sequence analysis of peptides was performed on an ABI 475A pulse liquid sequencer (Applied Biosystems). Data acquisition and analyses were performed with the standard program Run 470-I (ABI). The PTH amino acid HPLC separation protocol was slightly modified (trimethylamine was added to the normal A solvent as recommended by ABI for the separation of histidine and arginine) to allow for the identification of the PTH derivative of trimethyllysine.

RESULTS

Evidence That [^{3}H]2-N_3ADP Is Stably Trapped at the Active Site of S1. Several methods were used to establish that [^{3}H]2-N_3ADP was an appropriate analogue of ADP in its interaction with S1. The results in Figure 1 show there was a linear correlation between the loss of K^+EDTA ATPase activity and the trapping of [^{3}H]2-N_3ADP, indicating that [^{3}H]2-N_3ADP can be specifically trapped at the active site of S1. Typically, the fully inactivated enzyme trapped between 0.6 and 0.7 mol of [^{3}H]2-N_3ADP per mol of S1. Additional evidence that [^{3}H]2-N_3ADP was a useful analogue of ADP was its ability to enhance the inactivation of S1 by the bifunctional thiol cross-linking system Co(II)/Co(III) phenanthroline complexes (data not shown), which is known to occur only when nucleotides are trapped at the active site (Wells & Yount, 1979). In the absence of nucleotide, the $t_{1/2}$ of inactivation was 16 min as compared to 0.8 min in the presence of ADP and 1.2 min in the presence of 2-N_3ADP. Further evidence that [^{3}H]2-N_3ADP was specifically trapped at the active site is shown by the competition study in Figure 2. As the ratio of ADP to total nucleotide ([^{3}H]2-N_3ADP and ADP) was increased, the amount of trapped [^{3}H]2-N_3ADP/S1 was decreased in a linear fashion indicating that both nucleotides were competing for the same active site and that their affinities for the active site were similar.

Scheme I. Tautomers of 2-N_3ADP[a]

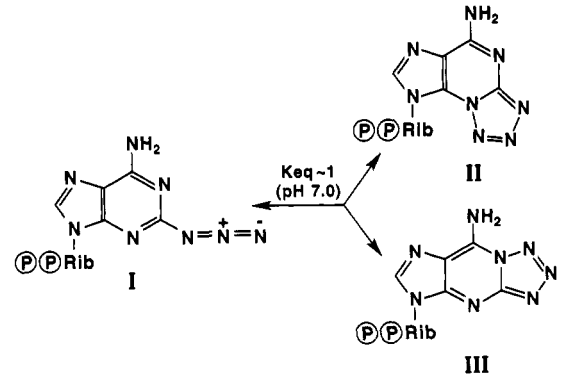

[a] (I) Azido isomer; (II) tetrazolo[5,1-*b*]adenosine; (III) tetrazolo[1,5-*a*]adenosine.

Photolabeling of S1 by [^{3}H]2-N_3ADP. The rate of photoincorporation of [^{3}H]2-N_3ADP into S1 is shown in Figure 3. By 2 min, the amount of photoincorporation was maximal at approximately 0.18 mol of [^{3}H]2-N_3ADP/mol of S1, which is equivalent to about 30% of the trapped nucleotide analogue (0.6 mol/mol of S1) being covalently incorporated. The low level of incorporation (~2%) observed in the untrapped control (no addition of $[Co(III)(phen)_2CO_3]^+$) was likely due to slow oxidation of the Co(II)phen·S1 complex by dissolved oxygen resulting in minor trapping of 2-N_3ADP.

In solution, 2-N_3ADP readily tautomerizes between the photolabile azido form and the two nonphotolabile tetrazolo isomers (see Scheme I; Czarnecki, 1984). It was of interest

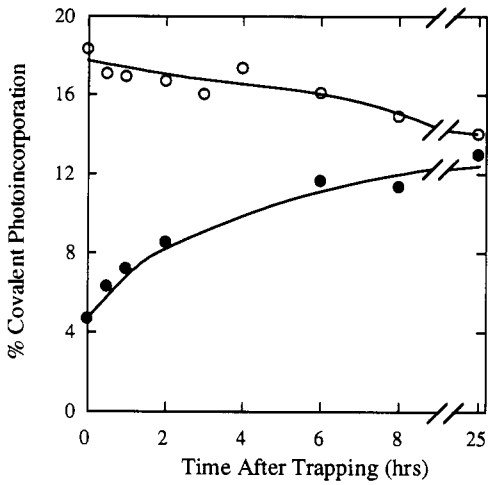

FIGURE 4: Photoincorporation of [^{3}H]2-N_3ADP into S1 vs time after trapping. [^{3}H]2-N_3ADP was incubated in either 0.1 N HCl (○, azido form) or 0.1 N NaOH (●, tetrazole form) for 15 h at 24 °C and neutralized with 1 M Tris, pH 8.0 immediately prior to use. S1 was inactivated and purified as described under Materials and Methods. At various times after trapping, the inactivated S1 was irradiated as described under Materials and Methods. Covalent incorporation of [^{3}H]2-N_3ADP into S1 was quantified as described in the legend to Figure 3.

to determine whether 2-N_3ADP trapped at the active site could tautomerize to the tetrazolo isomers at a rate to be of concern in labeling experiments. To test this possibility, the [^{3}H]2-N_3ADP·S1 trapped complex (0.6 mol/mol of S1) was allowed to sit on ice from 0.5 to 25 h prior to irradiation. As can be seen in Figure 4, the covalent photoincorporation (uncorrected for trapping) decreased only slightly from 18% initially to 14% after 25 h of incubation. This conclusion was confirmed by performing the reverse experiment in which 2-N_3ADP (converted to the tetrazolo isomers by prior treatment with 0.1 N NaOH) was trapped (0.6 mol/mol of S1) and irradiated over the same time span (Figure 4). Here, the initial photoincorporation was only 5% but gradually increased to 13% over 25 h. These results indicate that isomerization can occur at the active site. Moreover, the azido form of 2-N_3ADP is favored even though both the azido form and the tetrazolo forms were trapped with equal affinity initially. These results also show that the time required to purify the trapped 2-N_3ADP·S1 complex before irradiation (~30 min) decreased the percent of photoincorporation only marginally.

Subunit and Major Tryptic Fragment Localization of [^{3}H]2-N_3ADP Incorporation. The irradiated [^{3}H]2N_3-ADP·S1 complex was subjected to limited trypsin digestion to produce the characteristic NH_2-terminal 23-kDa, central 50-kDa, and COOH-terminal 20-kDa fragments of the S1 heavy chain (Balint et al., 1978). When analyzed by gel electrophoresis (Figure 5), all of the label, prior to trypsinization, was in the parent 95-kDa heavy chain fragment and none in the light chains. After 2 min of trypsinization, the label was seen primarily in the NH_2-terminal 75-kDa fragment and its 23-kDa cleavage product. The 20-kDa fragment was not labeled. As the digestion progressed, the labeling in the NH_2-terminal 23- kDa increased with a concurrent decrease in the 75-kDa precursor. A 10-kDa peptide, believed to come from the 23- kDa fragment, was also labeled. These results show that residues in the 23-kDa fragment are the major site of photolabeling.

Isolation of Photolabeled Peptides. The photolabeled S1 was digested with trypsin and subtilisin BPN′ as described under Materials and Methods. The labeled peptides were

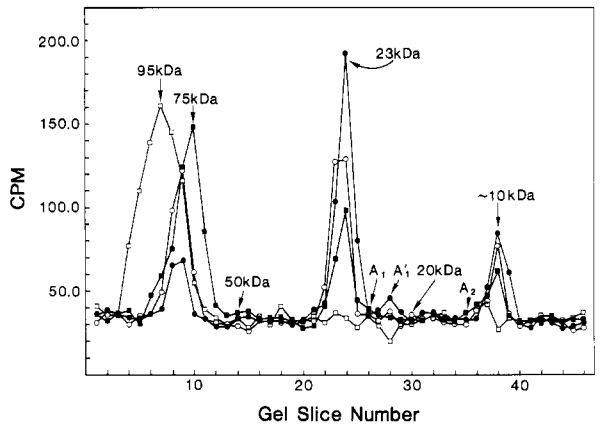

FIGURE 5: Localization of [^{3}H]2-N_3ADP labeling of S1 by limited tryptic digestion and SDS PAGE analysis. The S1·Mg[^{3}H]2-N_3ADP complex was prepared and irradiated as described under Materials and Methods and digested by 1/100 (w/w) trypsin. At various times, trypsin was inactivated by addition of SDS sample buffer and heating for 5 min at 98 °C (0 min, □; 2 min, ■; 5 min, ○; 10 min, ●). The tryptic fragments were separated on a 12% acrylamide, 0.32% bisacrylamide SDS gel (Laemmli, 1970). The gels were stained with 0.25% Coomassie Brilliant Blue G-250 in 45% MeOH, 45% H_2O, and 10% acetic acid overnight and destained in the same solvent without the dye. Radioactive tryptic fragments were localized by slicing each lane into 1.5-mm slices, followed by solubilization in 0.75 mL of H_2O_2/NH_4OH (99:1) at 60 °C for several hours (Albanese & Goodman, 1977). After neutralization with acetic acid, the slices were counted as described under Materials and Methods.

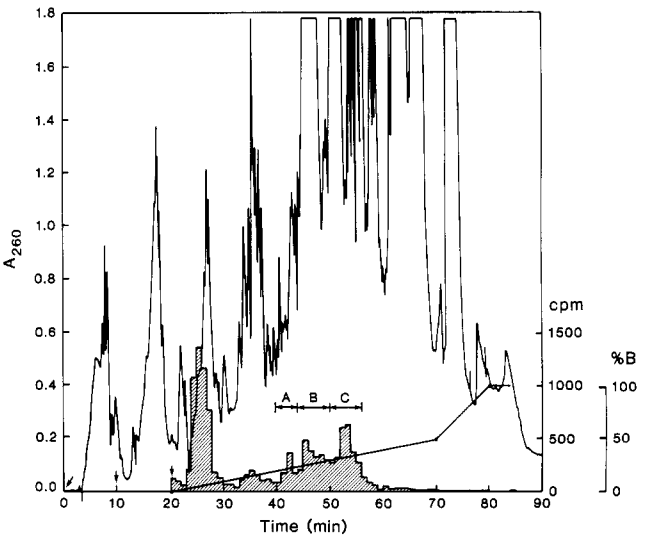

FIGURE 6: Semipreparative HPLC separations of a trypsin/subtilisin digest of photolabeled S1. S1 (200 mg) was photolabeled with [^{3}H]2-N_3ADP as described under Materials and Methods. Following digestion with trypsin and subtilisin as described under Materials and Methods, the digest was separated by three reversed-phase HPLC runs (66 mg per run) on a Brownlee C8 semipreparative column equilibrated in 5 mM KP_i, pH 6.9 . For each run, injections (↓) of 5.5 mL each (22 mg of digest/injection) at 0, 10, and 20 min were applied using a 7.5- mL loop . After the final injection, the column was developed with a 1%/min linear gradient of 5 mM KP_i, pH 6.9, to 65% CH_3CN/H_2O at a flow rate of 2 mL/min collecting 2-mL fractions. Aliquots (20 μL) of each fraction were analyzed for radioactivity (shaded area), and equivalent peptide pools (A, B, C) from the three runs were combined for further purification. The first 20 min of each run at 0% B was collected and contained the free, photolyzed [^{3}H]2-N_3ADP from the 0- and 10-min injections. The counts corresponding to the photolyzed [^{3}H]2-N_3ADP from the 20-min injection are shown on the graph.

initially separated by semipreparative C8 reversed-phase HPLC at neutral pH. As shown in Figure 6, the labeled peptides eluted as three major peaks: A, B and C (3%, 8%, and 10% of the recovered radioactivity, respectively). The

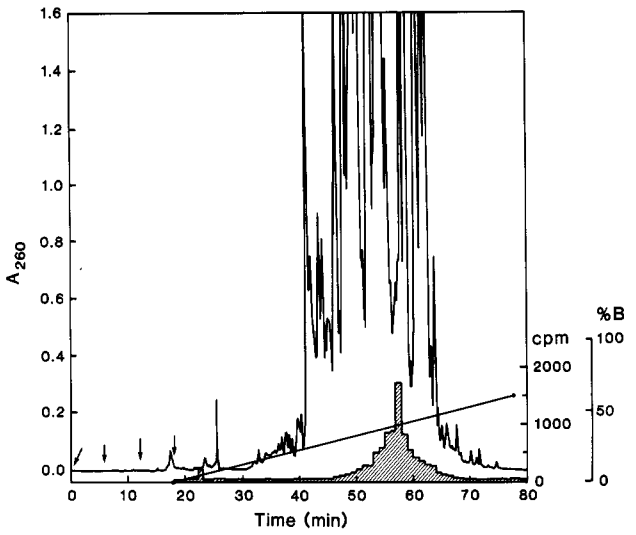

FIGURE 7: HPLC purification of peak B at pH 2.0. Fractions 45–50 (B) from each of the three initial separations (Figure 6) were pooled, concentrated on a SpeedVac (Savant, Farmingdale, NY), and applied to the column by multiple injections (↓) at 0, 6, 12, and 18 min on the C8 semipreparative column equilibrated in 0.11% TFA. Upon the final injection, the column was developed with a 1%/min gradient of 0.1% TFA/60% ACN at a flow rate of 2 mL/min collecting 2-mL fractions. An aliquot (20 μL) of each fraction was analyzed for radioactivity (shaded area). Total recovery of radioactivity was 97% with 96% of the recovered counts occurring in the broad peak between 47 and 68 min.

majority of the remainder of the recovered radioactivity (77%) was eluted in the combined void volumes of the three injections and represents free, photolyzed [^{3}H]2-N_3ADP which was trapped but not covalently incorporated into S1. The radioactive profile from only the final injection is shown. The distribution of radioactivity is consistent with the level of photoincorporation (~25 %) determined for this sample.

The radioactive peptides which eluted between 45 and 50 min (peak B) were pooled and further purified on the same column at pH 2 using a TFA/CH_3CN system (Figure 7). Over 96% of the recovered radioactivity eluted in a broad peak between 46 and 67 min. The remaining 3% eluted in the void volume (0–30 min). Peptide peak C from the first reversed-phase separation (Figure 6) was also purified in a similar manner (data not shown). In this latter case, all of the recovered radioactivity eluted between 34 and 54% solvent B and appeared to contain at least three labeled peptides. These three peptide pools (C1, C2, and C3) were collected for further purification (see below). Peak A (Figure 6) was not examined further because it contained the lowest level of radioactivity.

Because the photolabeled peptides contained the negatively charged diphosphate moiety, we used anion exchange HPLC for the next stage of purification. Peptides from pool B (Figure 7) were applied to an AX300 column at pH 8.0 (Figure 8). The majority of the unlabeled peptides were either not retained or eluted early in the salt gradient. In contrast, the radioactive peptides were retained and eluted as a broad, bimodal peak between 40 and 68 min. The peak was split into two pools, B1 (46–54 min) and B2 (55–68 min), for further purification. Peptides from C1 and C2 (see above) were also purified in this manner (data not shown). In both cases, all recovered radioactivity was eluted late in the gradient whereas the majority of the unlabeled peptides were eluted either before or shortly after initiation of the gradient. Both separations gave broad, polymodal peaks, and therefore C1 was separated into three fractions (C1a, C1b, and C1c) and C2 into two fractions (C2a and C2b) for further purification. All of these pooled fractions were desalted on an analytical C8 column using the TFA/CH_3CN system (data not shown) and taken to dryness in a SpeedVac concentrator.

For the final step in the purification, these peptides were treated with *Escherichia coli* alkaline phosphatase for two reasons. First, removal of the phosphate groups from the photolabeled peptides drastically alters their retention time on reversed- phase HPLC, facilitating their final purification, and, second, it facilitates the extraction of the PTH derivative of the radioactive photolabeled amino acid during subsequent

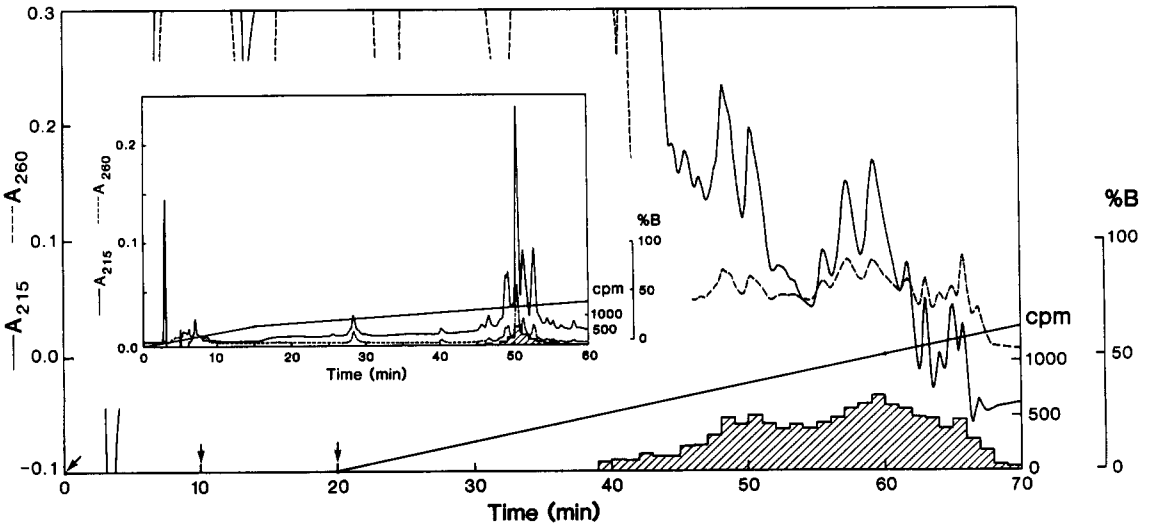

FIGURE 8: Anion exchange HPLC separation of peak B peptides (Figure 7). Fractions 52–64 were concentrated as described in the Figure 7 legend, adjusted to pH 8.0 with 1 M Tris (free base), and loaded by multiple injections (↓) at 0, 10, and 20 min onto a Brownlee AX300 column (4.5 mm × 13 cm) equilibrated in 20 mM Tris, pH 8.0. Upon the final injection, the column was developed by a linear gradient to 20 mM Tris, pH 8.0, and 2 M NaCl over 80 min at a flow rate of 1 mL/min. Fractions were collected and analyzed as described in the legend to Figure 7. Fractions 46–54 (32% of recovered radioactivity) were pooled as peptide B1, and fractions 55–68 (62% of recovered counts) were pooled as peptide B2. (Inset) Alkaline phosphatase treatment and HPLC purification of peptide B2. Peptide B2 was desalted by analytical C8 HPLC using the TFA/CH_3CN system (Figure 7) and taken to dryness (SpeedVac). The peptide (5 nmol) was resuspended in 0.5 mL of 100 mM Tris, pH 8.0, and 1 mM $MgCl_2$, and 2.8 units of *E. coli* alkaline phosphatase (Sigma) was added. After incubation at room temperature for 16 h, the sample was purified on the C8 analytical column using the TFA/CH_3CN system (Figure 7) with the gradient as shown at 1 mL/min. The major radioactive peptide, fraction 51, was used for sequence analysis.

Table I: Sequence Analysis of the Major Photolabeled Peptides from [^{3}H]2-N_3ADP-S1

amino acid	amino acid yield (pmol)[b]							
	B1 (53′)[a]	B2 (51′)	C1a (55′)	C1b (58′)	C2a (64′)	C2a (66′)	C2b (63′)	C2b (64′)
V			120	139	133	156		
N			75	148	131	153		
P			108	189	172	188		
Y			115	189	161	189		
TMK	177	150	86	105	82	140	182	221
X[c]	nil	nil	nil	nil	nil	nil	nil	nil
L	377	351	50	113	54	55	106	141
P	362	262	53	124	73	58	61	105
V	303	311	23	80	38	37	25	102
Y	274	225	26	112	48	48	3.5	85
N	193	169	12	84	23	36		51
P	175	211	2	75	17	35		45
E	27	37		10	4	5		12

[a] The number in parentheses refers to the retention time on the final HPLC desalting run of the peak used for sequence analysis. [b] Picomole yield of PTH amino acids. [c] "X" is Trp-130 as deduced from the primary amino acid sequence of rabbit skeletal myosin heavy chain (Tong & Elzinga, 1983).

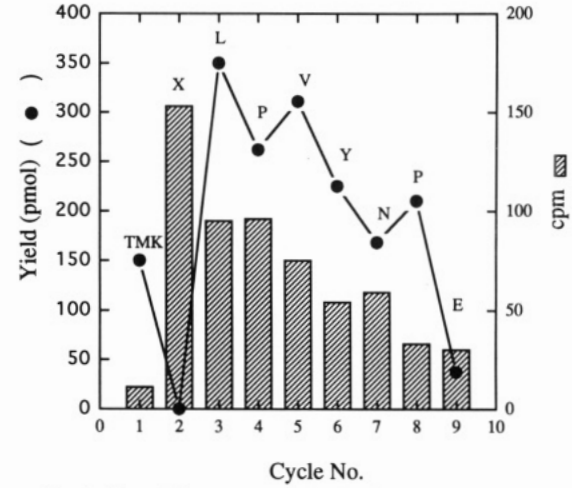

FIGURE 9: Amino acid sequence analysis of peptide B2. The peptide was sequenced as described under Materials and Methods, and the fractions containing the extracted PTH amino acids were analyzed for radioactivity. TMK is trimethyllysine.

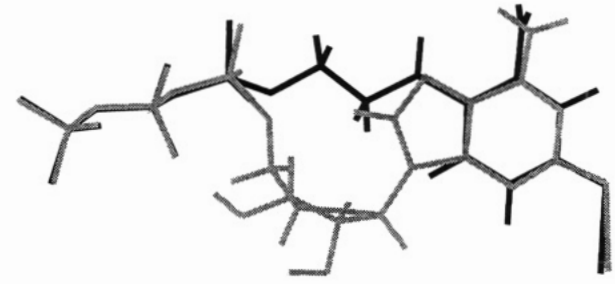

FIGURE 10: Computer generated structures of 2-N_3ATP (gray) and NANTP (black) showing how their azido groups (far right) are superimposable in extended conformation. Biosym programs Insight II (version 2.1.0, Biosym Technologies, Inc., San Diego, CA, 1992) and Discover (version 2.8, Biosym Technologies, Inc., San Diego, CA, 1992) were used to build and minimize both models. The Discover TemplateForce subroutine was used to overlay the two models by superimposing the α, β, and γ phosphates and 2, 4, and 6 carbons of each model during a series of minimizations. The azido bond lengths and geometries came from the crystal structures of several aromatic azides located in the Cambridge Structural Database (Allen et al., 1983).

peptide sequence analysis. Thus, the site of photolabeling can be directly identified. After treatment with alkaline phosphatase, peptide B2 was further purified by analytical C8 HPLC using a TFA/CH_3CN system (Figure 8, inset). Several radioactive peptides were identified, and the major one which eluted at 51 min was submitted for sequence analysis. Peptides B1, C1a, C1b, C2a, and C2b were also treated with alkaline phosphatase and purified in this manner. In each case, several radioactive peptides were purified from each separation, and the major peptide peaks were analyzed for their amino acid sequence.

Amino Acid Sequence Analysis. The amino acid sequence of peptide B2 (eluting at 51 min) was found to be TMK_{129}-X-L-P-V-Y-N-P-E_{137} (Figure 9). The missing residue at cycle 2 corresponds to Trp-130 in the rabbit skeletal myosin sequence (Tong & Elzinga, 1983). The radioactivity was first released at cycle 2, indicating Trp-130 as the site of photomodification. The radioactivity in cycles after cycle 2 are thought to be the result of incomplete extraction of the modified Trp-130 PTH derivative. The phenylthiohydantoin derivative of trimethyllysine (TMK) was specifically identified by a modification of the ABI HPLC separation protocol as described under Materials and Methods. Table I shows the sequence of the other seven peptides analyzed. In each case, Trp-130 was the only missing amino acid, and the radioactivity was first released with this cycle. Two sets of the peptides appeared to be the same by sequence analysis, e.g., (1) B_1, B_2, and C_{2b} (64′), and (2) C_{1b} and C_{2a} (64′ and 66′), despite their different behavior on HPLC separations. Some of these differences may reflect additional amino acids beyond Glu-137 (the last residue analyzed), or it may reflect incomplete removal of the two phosphates on the attached photoprobe by alkaline phosphatase treatment.

DISCUSSION

The purpose of this study was to characterize the amino acid residues of skeletal myosin which bind at or near the adenine ring of ATP. 2-N_3ATP was chosen for this purpose because in preliminary studies we found it gave higher photoincorporation levels than the more extensively studied 8-N_3ATP. Similar results have been observed in comparable studies with these two photoprobes with the F_1 ATPase from mitochondria (Garin et al., 1986; Xue et al., 1987; Cross et al., 1987; Hartog et al., 1992) and from chloroplasts (Czarnecki et al., 1982; Xue et al., 1988). The lower photoincorporation with 8-N_3ATP may reflect the fact that, at least with mitochondrial F_1 ATPase, ATP and 8-N_3ATP are known from NMR studies to bind in the *anti* conformation (Garin et al., 1988). Here, the binding energy of the active site for the *anti* conformation of ATP (and 8-N_3ATP) is enough to overcome the steric factors which in solution favor the *syn* conformation of 8-substituted ATP derivatives (Sarma et al., 1974). The *anti* conformation of 8-N_3ATP places the 8-azido group directly over the ribose ring with which it could easily react after photolysis. Alternatively, the ribose ring may simply block access of the 8-azido group to neighboring amino acids but not block access to water. Either explanation could rationalize the low photoincorporation of this analogue with energy-transducing ATPases.

In contrast, 2-N_3ATP used in this study (see Figure 10) has the 2-azido group pointing away from the ribose ring when in the *anti* conformation. As shown in Figure 10, both 2-N_3ATP and NANTP can exist in conformations in which their triphosphate moieties and azido groups can be superimposed. We have previously shown (Okamoto & Yount, 1985) that NANDP specifically photolabels Trp-130. The fact that 2-N_3ADP also photolabels Trp-130 suggests that

the analogue conformations shown in Figure 10 are likely close to their myosin-bound conformations. We have been unable, either with computer modeling or with CPK models, to find other conformations which allow both the phosphate groups and the azido groups of NANTP and 2-N_3ATP to be superimposed. That the *anti* position for ATP on myosin appears to be favored is not surprising because a large number of purine nucleotides bind to enzymes with known crystal structures in this conformation (Brunie et al., 1990; Kabsch et al., 1990; Pai et al., 1990; Rould et al., 1989).

The ability of 2-N_3ATP to serve as an effective photoaffinity label is potentially decreased by its property of rearranging into nonphotoreactive tetrazoles at neutral or basic pH values (Scheme I; see Czarnecki, 1984 and references therein). Fortunately, the azido form is favored at low pH values and in nonpolar solvents, so that, by preincubation of 2-N_3ATP or 2-N_3ADP at pH 1–2 immediately before neutralizing the solution and photolysis, the large majority of the analogue is in the azido form. The isomerization of the azido form at pH 7.0 to the tetrazolo isomers is generally slow enough ($t_{1/2} \sim$ 30 min at 25 °C; Czarnecki, 1984) that effective photoincorporation can occur. Here we were able to observe this isomerization at the active site of myosin by trapping, alternatively, the azido- and tetrazolo- forms of 2-N_3ADP and measuring the photoincorporation as a function of time. As shown in Figure 4, photoincorporation of the trapped azido species decreased very little over 25 h (18–14%) while that of the tetrazolo isomers was initially low (5%) and grew to 13% over the same time period. These results suggest the purine portion of the active site is relatively hydrophobic, a property favoring the azido isomer. This result is in agreement with earlier spectroscopic studies with NANTP which indicated a polarity at the purine site equal to 60% ethanol (Nakamaye et al., 1985).

The importance of using some form of "active site trapping" to stabilize nucleotide analogue binding on myosin before photoaffinity labeling cannot be overemphasized. There are now several methods to trap ADP or ADP analogues at the active site of myosin. These methods for skeletal myosin include cross-linking SH_1 (Cys-707) and SH_2 (Cys-697) by complexation with Co(III)phen (Wells & Yount, 1979) or by reaction with bifunctional cross-linkers, such as *p*-phenylenedimaleimide [Burke & Reisler, 1977; reviewed in Wells and Yount (1982)]. Other trapping methods include forming stable transition state-like complexes with nucleoside diphosphates and phosphate analogues such as vanadate (Goodno, 1979), BeF_3^- (Phan & Reisler, 1992), or AlF_4^- (Werber et al., 1992). These methods typically give complexes with half-lives of days at 0 °C and allow the complexes to be purified free of extraneous photoaffinity analogue before irradiation. Here we used the Co(III)phen system because it is the fastest of the above trapping methods and it allowed us to purify and irradiate the 2-N_3ADP·S_1 complex before significant isomerization to the tetrazolo forms could occur. We observed here as we have reported previously (Nakamaye et al., 1985; Mahmood et al., 1989; Cole & Yount, 1990) that nontrapped ATP photoaffinity analogues in reaction with S1 tend to photolabel all three major heavy chain tryptic peptides (23, 50, and 20 kDa). When trapped, both 8-N_3ADP and 2-N_3ADP labeled only the 23-kDa NH_2-terminal fragment. These results may partially explain the observation of Maruta et al. (1989) that a fluorescent derivative of 8-N_3ATP photolabeled predominantly the 20-kDa heavy chain tryptic fragment with some labeling of the 50-kDa fragment. In these experiments, no trapping method was used, and it is possible that some of the photolabeling observed was nonspecific. Further evidence for nonspecific labeling was the fact ATP did not protect against labeling nor was the photolabeled enzyme inactivated. It is important to recognize that trapping with 8-N_3ATP is a factor of 4–5 times slower than with other analogues. The major problem with 8-N_3ATP photolabeling of myosin even when trapped is the low photoincorporation and the subsequent instability of the photolabeled adduct(s) to normal HPLC purification methods.

Two techniques were critical in our purification of pure [^{3}H]2-N_3ADP labeled peptides. These were (i) the use of anion-exchange chromatography to separate peptides containing diphosphate groups from other less anionic peptides which had copurified during prior reversed-phase HPLC runs. This method introduced by Evans et al. (1989) appears to be a generally useful major purification step for peptides with nucleotide photolabels attached and complements the use of Fe chelate columns for the same purpose (Salvucci et al., 1992). The second method (ii) was the enzymatic removal of the two phosphate groups from photolabeled peptides with *E. coli* alkaline phosphatase (Garabedian & Yount, 1991). This treatment leaves only the [^{3}H]nucleoside attached to the peptide and again generates peptides with chromatographic properties much different from those of contaminating peptides. This approach has the disadvantage that ^{32}P-labeled analogues cannot be used. However, the removal of the phosphates allowed the [^{3}H]nucleoside–amino acid–PTH adduct to be extracted during the normal gas phase sequencing cycle and its radioactivity determined directly. Normally, if the phosphate groups are on the nucleoside, the labeled amino acid PTH derivative remains bound to the sequencing filter. Thus we were able to show the majority of the radioactivity was released and extracted at the cycle corresponding to Trp-130. The correctness of this identification as Trp-130 was furthered by the positive identification of trimethyllysine (TMK-129) at the cycle immediately preceding the release of radioactivity (Table I).

The role of Trp-130 in the ATPase activity of myosin is unclear. The recent observation (Peyser et al., 1990) that Trp-130 can be modified with the reagent dimethyl(2-hydroxy-5-nitrobenzyl)sulfonium bromide (DHNBS) while having little effect on the actin-activated MgATPase (Werber et al., 1987) indicates it cannot play a critical role. However, the chemistry of the DHNBS reaction with tryptophan is not known, and it is possible that its adduct with the indole ring of tryptophan still allows myosin to function normally as an ATPase. While Trp-130 is highly conserved among skeletal myosins, it is replaced by Asn in yeast (Watts et al., 1987), by Gln in gizzard myosin (Yanagisawa et al., 1987), and by Arg in scallop (Nyitray et al., 1991) acanthamoeba (Hammer et al., 1987), nematode (Karn et al., 1983), and dictyostelium myosins (Warrick et al., 1986). This indicates Trp cannot be essential for ATP hydrolysis. It is, however, important to point out that NANDP specifically photolabels Arg-128 in high yield when trapped on scallop myosin (Kerwin & Yount, 1992). This Arg, as noted above, is in the same sequence location in the heavy chain of scallop myosin as Trp-130 is in rabbit skeletal myosin. Thus, it is extremely unlikely that this Arg is also simply the most reactive Arg on the surface of myosin (as Trp-130 appears to be) and that is why it is photolabeled.

In conclusion, all our photolabeling evidence to date is consistent with the adenine-binding site being located primarily on the 23-kDa heavy chain fragment. The fact that Trp-130 in this fragment is photolabeled specifically by two active site-trapped ADP analogues in high yields gives strong evidence

that it contributes to the adenine-binding site of ATP on myosin. The exact nature of the interaction of Trp-130 with ATP awaits the solution of the crystal structure of an S1·ATP complex.

ACKNOWLEDGMENT

We are indebted to Dr. J. Czarnecki for a gift of 2-N_3ATP and [^{3}H]2-N_3ATP and for his advice in the early stages of this work. We thank Dr. Gerhard Munske of the WSU Laboratory for Bioanalysis and Biotechnology for sequencing the peptides, David Lawson for generating the computer models of 2-N_3ATP and NANTP, and Drs. Christine Cremo and Bruce Kerwin for their critical comments on the manuscript.

REFERENCES

Albanese, E., & Goodman, D. (1977) *Anal. Biochem. 80*, 60–69.
Allen, F. H., Kennard, O., & Taylor, R. (1983) *Acc. Chem. Res. 16*, 146–153.
Atkinson, M. A., Robinson, E. A., Appella, E., & Korn, E. D. (1986) *J. Biol. Chem. 261*, 1844–1848.
Balint, M., Wolf, I., Tarcsafalvi, A., Gergely, J., & Sreter, F. A. (1978) *Arch. Biochem. Biophys. 190*, 793–799.
Bradford, M. M. (1976) *Anal. Biochem. 72*, 248–254.
Bridenbaugh, R. L. (1980) Ph.D. Thesis, Washington Sate University, Pullman, WA.
Brunie, S., Zelwer, C., & Risler, J.-L. (1990) *J. Mol. Biol. 216*, 411–424.
Burke, M., & Reisler, E. (1977) *Biochemistry 16*, 5559–5563.
Cole, D. G., & Yount, R. G. (1990) *J. Biol. Chem. 265*, 22537–22546.
Cremo, C. R., Grammer, J. C., & Yount, R. G. (1989) *J. Biol. Chem. 264*, 6608–6611.
Cross, R. L., Cunningham, D., Miller, C. G., Xue, Z., Zhou, Z.-M., & Boyer, P. D. (1987) *Proc. Natl. Acad. Sci. U.S.A. 84*, 5715–5719.
Czarnecki, J. J. (1984) *Biochim. Biophys. Acta 800*, 41–51.
Czarnecki, J. J., Abbott, M. S., & Selman, B. R. (1982) *Proc. Natl. Acad. Sci. U.S.A. 79*, 7744–7748.
Evans, R. K., Beach, C. M., & Coleman, M. S. (1989) *Biochemistry 28*, 713–720.
Garabedian, T., & Yount, R. G. (1990) *J. Biol. Chem. 265*, 22547–22553.
Garabedian, T., & Yount, R. G. (1991) *Biochemistry 30*, 10126–10132.
Garin, J., Boulay, F., Issartel, J. P., Lunardi, J., & Vignais, P. V. (1986) *Biochemistry 25*, 4431–4437.
Garin, J., Vignais, P. F., Gronenborn, A. M., Clore, G. M., Gao, Z., & Baeuerlein, E. (1988) *FEBS Lett. 242*, 178–182.
Goodno, C. (1979) *Proc. Natl. Acad. Sci. U.S.A. 76*, 2620–2624.
Grammer, J. C., & Yount, R. G. (1991) *Biophys. J. 59*, 226a.
Grammer, J. C., Cremo, C. R., & Yount, R. G. (1988) *Biochemistry 27*, 8408–8415.
Haley, B. E., & Hoffman, J. F. (1974) *Proc. Natl. Acad. Sci. U.S.A. 71*, 3367–3371.
Hammer, J. A., III, Bowers, B., Paterson, B. M., & Korn, E. D. (1987) *J. Cell Biol. 105*, 913–925.
Hartog, A. F., Edel, C. M., Lubbers, F. B., & Berden, J. A. (1992) *Biochim. Biophys. Acta 1100*, 267–277.
Kabsch, W., Mannherz, H. G., Suck, D., Pai, E. F., & Holmes, K. C. (1990) *Nature 347*, 37–44.
Karn, J., Brenner, S., & Barnett, L. (1983) *Proc. Natl. Acad. Sci. U.S.A. 80*, 4253–4257.
Kerwin, B. A., & Yount, R. G. (1992) *Bioconjugate Chem. 3*, 328–336.
Laemmli, U. K. (1970) *Nature 227*, 680–685.
Mahmood, R., Elzinga, M., & Yount, R. G. (1989) *Biochemistry 28*, 3989–3995.
Maruta, S., Miyanishi, T., & Matsuda, G. (1989) *Eur. J. Biochem. 184*, 213–221.
Nakamaye, K. L., Wells, J. A., Bridenbaugh, R. L., Okamoto, Y., & Yount, R. G. (1985) *Biochemistry 24*, 5226–5235.
Nyitray, L., Goodwin, E. B., & Szent-Györgyi, A. G. (1991) *J. Biol. Chem. 266*, 18469–18476.
Okamoto, Y., & Sekine, T. (1985) *J. Biochem. (Tokyo) 98*, 1143–1145.
Okamoto, Y., & Yount, R. G. (1985) *Proc. Natl. Acad. Sci. U.S.A. 82*, 1575–1579.
Pai, E. F., Krengel, U., Petsko, G. A., Goody, R. S., Kabsch, W., & Wittinghofer, A. (1990) *EMBO J. 9*, 2351–2359.
Pate, E., Nakamaye, K. L., Franks-Skiba, K., Yount, R. G., & Cooke, R. (1991) *Biophys. J. 59*, 598–605.
Peyser, Y. M., Muhlrad, A., & Werber, M. M. (1990) *FEBS Lett. 259*, 346–348.
Phan, B., & Reisler, E. (1992) *Biochemistry 31*, 4787–4793.
Riquelme, P. T., & Czarnecki, J. J. (1983) *J. Biol. Chem. 258*, 8240–8245.
Rould, M. A., Perona, J. J., Soll, D., & Steitz, T. A. (1989) *Science 246*, 1135–1142.
Salvucci, M. E., Chavan, A. J., & Haley, B. E. (1992) *Biochemistry 31*, 4479–4487.
Sarma, R. H., Lee, C. H., Evans, F. E., Yathrinda, N., & Sundaralingam, M. (1974) *J. Am. Chem. Soc. 96*, 7337–7348.
Sutoh, K. (1987) *Biochemistry 26*, 7648–7654.
Tong, S. W., & Elzinga, M. (1983) *J. Biol. Chem. 258*, 13100–13110.
Wagner, P. D., & Yount, R. G. (1975) *Biochemistry 14*, 1900–1907.
Wagner, P. D., & Weeds, A. (1977) *J. Mol. Biol. 109*, 455–473.
Warrick, H. M., De Lozanne, A., Leinwand, L., & Spudich, J. A. (1986) *Proc. Natl. Acad. Sci. U.S.A. 83*, 9433–9437.
Watts, F. Z., Shiels, G., & Orr, E. (1987) *EMBO J. 6*, 3499–3505.
Wells, J. A., & Yount, R. G. (1979) *Proc. Natl. Acad. Sci. U.S.A. 76*, 4966–4970.
Wells, J. A., & Yount, R. G. (1982) *Methods Enzymol. 85*, 93–116.
Wells, J. A., Werber, M. M., & Yount, R. G. (1979a) *Biochemistry 18*, 4800–4805.
Wells, J. A., Werber, M. M., Legg, J. I., & Yount, R. G. (1979b) *Biochemistry 18*, 4793–4799.
Werber, M. M., Peyser, Y. M., & Muhlrad, A. (1987) *Biochemistry 26*, 2903–2909.
Werber, M. M., Peyser, Y. M., & Muhlrad, A. (1992) *Biochemistry 31*, 7190–7197.
Xue, Z., Miller, C. G., Zhou, J.-M., & Boyer, P. D. (1987) *FEBS Lett. 223*, 391–394.
Xue, Z., Melese, T., Stempel, K. E., Reedy, T. J., & Boyer, P. D. (1988) *J. Biol. Chem. 263*, 16880–16885.
Yanagisawa, M., Hamada, Y., Katsuraguwa, Y., Imamura, M., Mikawa, T., & Masaki, T. (1987) *J. Mol. Biol. 198*, 143–157.
Yount, R. G., Cremo, C. R., Grammer, J. C., & Kerwin, B. A. (1992) *Phil. Trans. R. Soc. London B 336*, 55–61.